Modified boost converter for renewable energy powered battery charger

Amrita Kushwaha[1] [ID], Arif Iqbal[2*] [ID] and M. Arifuddin Mallick[1] [ID]

[1, 3]*Department of Electrical Engineering, Integral University, Lucknow, 226026, India*
[2]*Department of Electrical Engineering, Rajkiya Engineering College, Ambedkar Nagar, 224122, India*

Abstract

In view of the tremendous electrification of transportation sector, development and management of an integrated charging unit has been under research focus for last few decades. Therefore, this paper deals with the development of an integrated battery charging unit in which a modified DC-DC boost converter has been proposed for electric vehicles (EVs). With a nominal number of components (one inductor, one capacitor, one diode and three switches) in proposed converter, charging unit is suitable to charge the batteries in a wide voltage range. A simplified control scheme is also developed to regulate the output DC link voltage of proposed converter which is used to charge a connected battery during plug-in operation. Propulsion system is developed by using a three phase induction machine (as propulsion motor) of vehicle, which has been controlled by using indirect field-oriented scheme to ensure higher performance. Operation of the motor drive has been investigated during propulsion and regeneration operation. Complete system has been developed and investigated by using Matlab/Simulink.

Keywords: Battery charger; Boost converter; Electric vehicles; Propulsion motor

To cite this paper: Kushwaha, A., Iqbal, A., Mallick, M. A., Modified boost converter for renewable energy powered battery charger. International Journal of Automotive Science and Technology. 2024; 8(1): 30-36. http://dx.doi.org/10.30939/ijastech..1379486

1. Introduction

With the ever increasing energy demand together with the various environmental issues, there is a steady shift of conventional energy source to renewable side for last few decades. Use of renewable energy has revolutionized many industrial sectors. In this regard, many advanced findings have been presented showing a tremendous development transportation domain. It is expected that conventional vehicles will be electric vehicles (EVs) and hybrid EVs in near future [1, 2]. With the on-going deployment of renewable energy in automobile sector has increased the usage of EVs. But, it is accompanied by various challenges including the efficient charging unit using an advanced control scheme and infrastructure [3-5]. For battery charging purpose, input supply are usually transformed in single or double stages and hence, identified as single stage or two stage charger respectively. For higher power application, two-stage charger is used with a low output harmonics [6, 7]. Although, such charger is suitable for high density battery but, structurally it is more complex due to higher number of components and complicated control schemes. Single stage charger on other hand, uses a less number of components [8-11] and is suited

with the available DC grids and renewable energy resources [12, 13].

With the development in the field of power electronics and advanced control system, provided an opportunity to different electrical motors in propulsion system of EVs. Desirable features of the propulsion motor are: ability to generate higher starting torque, higher efficiency, smaller size, lower operational noise and cost effectiveness. [14, 15]. For small power application, DC motor is used, which yield high starting torque with simple control. But, it offers the disadvantage of frequent maintenance and high noise due to the use of commutator and brush arrangement [16]. In view of it, Brushless DC (BLDC) motor is now replacing the conventional DC motor which uses the electronic commutator, requiring less maintenance [15, 16]. Presently, Permanent Magnet Synchronous Motor (PMSM) is preferably used in automobile vehicle, suited for high performance and higher power application [17]. It uses the PM and characterized by back electromotive force (emf) which is sinusoidal in nature but, is trapezoidal in shape in case of BLDC motor. Major challenge in PMSM is due to the high cost of magnets used, which may be further demagnetized at higher current flow in stator winding. These factors need to be addressed

without scarifying the performance of EVs [14, 16-18]. Among the PM free propulsion motor, induction machine has been successfully used in transportation sector [19] due to their mature control technologies, negligible maintenance, robust construction, availability in wide power range and low cost. In view of these features, a three-phase induction motor has been considered in propulsion of present work.

This paper presents a modified DC-DC boost converter topology to develop an integrated battery charger of EVs. A simplified control scheme of proposed converter is also developed to regulate the output DC link voltage, used to charge the battery during plug-in operation. Investigated EV system is equipped with a three-phase induction machine as a propulsion motor which is controlled by using indirect field oriented scheme to ensure high performance of propulsion system. Operation of the propulsion motor has been presented during propulsion and regeneration of vehicle. Complete system has been developed and simulated by using Matlab/Simulink. Remaining sections of this paper are organized as: Section 2 presents the mathematical modeling of a three-phase propulsion motor. In section 3, operation of proposed modified boost converter is presented in all operating modes: plug-in, propulsion and regeneration. Section 4 presents the employed control scheme applicable to proposed converter and drive unit of motor. Section 5 presents a discussion on the obtained results in different modes of operation. Finally in section 6, concluding key remarks are presented obtained during the analysis of developed system.

2. Mathematical model of propulsion motor

In the propulsion system, a three-phase induction machine has been considered as propulsion motor. In arbitrary reference frame at speed ω_k, both stator and rotor circuit are mathematically defined as [20]:

$$v_{qds} = R_s i_{qds} + \omega_k F_{dqs} + pF_{qds} \tag{1}$$

$$v_{qdr} = R_r i_{qdr} + (\omega_k - \omega_r)F_{dqr} + pF_{qdr} \tag{2}$$

where, $v_{qds} = [v_{qs} \quad v_{ds}]^T$; $v_{qdr} = [v_{qr} \quad v_{dr}]^T$

$i_{qds} = [i_{qs} \quad i_{ds}]^T$; $i_{qdr} = [i_{qr} \quad i_{dr}]^T$

$F_{qds} = [F_{qs} \quad F_{ds}]^T$; $F_{qdr} = [F_{qr} \quad F_{dr}]^T$

$F_{dqs} = [F_{ds} \quad -F_{qs}]^T$; $F_{dqr} = [F_{dr} \quad -F_{qr}]^T$

In above expressions having the subscript 's' and 'r' show the quantity of stator and rotor respectively. Flux linkage F of stator and rotor in two axis coordinate system (d-q) is defined as

$$F_{dqs} = L_{ls}i_{dqs} + L_m(i_{dqs} + i_{dqr}) \tag{3}$$

$$F_{dqr} = L_{lr}i_{dqr} + L_m(i_{dqs} + i_{dqr}) \tag{4}$$

Developed motor torque and rotor speed are;

$$T_e = \left(\frac{3}{2}\right)\left(\frac{P}{2}\right)\left(F_{ds}i_{qs} - F_{qs}i_{ds}\right) \tag{5}$$

$$\omega_r = \frac{P}{2J}\int(T_e - T_l)dt \tag{6}$$

wherein P, J and T_l denotes the number of poles, moment of inertia and load torque respectively.

3. Proposed converter operation

In the proposed converter topology, the DC input is given from renewable energy source (solar PV, fuel cell etc.) and is designated as Renewable Energy Side Converter (RESC). This converter is used to obtain the boosted DC output which is fed to the machine drive unit (MDU) of propulsion motor. The proposed RECS is a modified DC-DC boost converter, constituted by a nominal number of components i.e. three switches (i.e. S_1, S_2, S_3), one diode, one inductor (L) and one capacitor (C). This also signifies a simple and easy design of proposed converter. Proposed RESC used in an integrated battery charging unit of EVs operates in the following modes:

3.1 Plug-in operation

The developed charging unit is connected to the DC source during plug-in operation. Charging of the connected battery takes
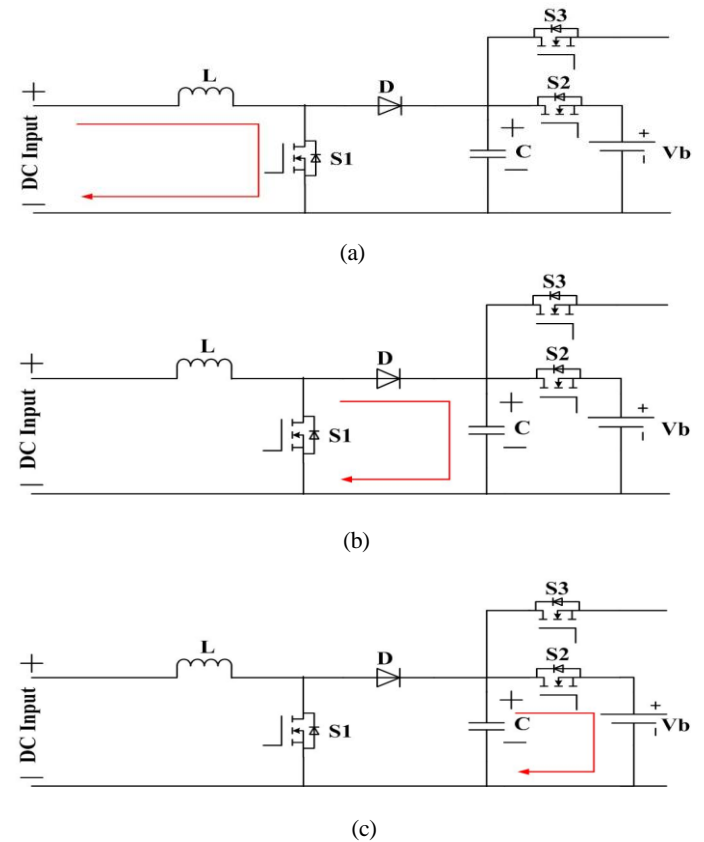

Fig. 1. Plug-in operation during (a) Stage I (b) Stage II (c) Stage III

place in different stages. In stage I, energy from DC source is transferred to the connected inductor (L) through switch S_1 and current flows through the path: $V^+ - L - S_1 - V^-$, transferring energy from DC source to indictor L. Flow of current in stage I is shown by red arrow in Fig. 1 (a). In stage II, inductor stored energy is transferred to the capacitor C by the flow of current in the path: $V^+ - L - D - C^+ - C^- - V^-$, hence increases the voltage v_C. Flow of current in stage II is shown by red arrow in Fig. 1 (b). In stage III, this energy stored in capacitor C is used to charge the connected battery through the flow of current in the path: $C^+ - S_2 - V_b^+ - V_b^- - C^-$ hence, increases the voltage V_b. Flow of current in stage III is shown by red arrow in Fig. 1 (c). Associated voltage and current waveforms during plug-in operation are shown in Fig. 4 (a).

3.2 Propulsion operation

During this operation, DC power stored in battery is used to drive the propulsion motor through inverter circuit. Initially at stage I, switch S_3 is operated ($S_3 = 1$) and current flows to transfer the stored energy of capacitor through the path: $C^+ - S_3 - MDU - C^-$. This decreases the capacitor voltage v_C. In stage II, the voltage v_C is restored through the transfer of the stored battery energy to capacitor by the flow of current in path: $V_b^+ - S_2 - C^+ - C^- - V_b^-$. Flow of current path in stage I and II is shown in Fig. 2 (a) and Fig. 2 (b) respectively. Voltage-current waveforms during propulsion operation are shown in Fig. 4 (b).

3.3 Regeneration operation

During this operation, energy is fed back to the battery from drive unit of propulsion motor. During stage I, switch S_3 is in ON position ($S_3 = 1$) and current flows in the path $MDU - S_3 - C^+ - C^- - MDU$. This results an increase in capacitor voltage v_C and hence, increases the stored energy in it.
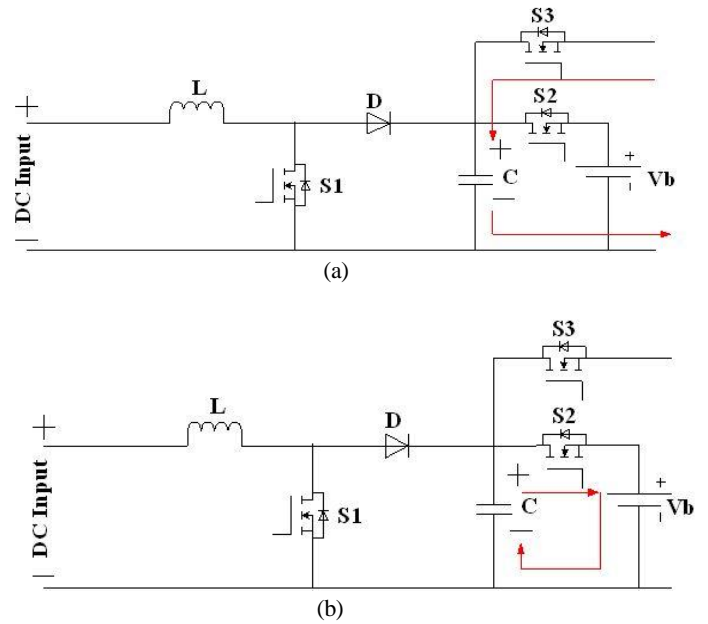

(a)

(b)

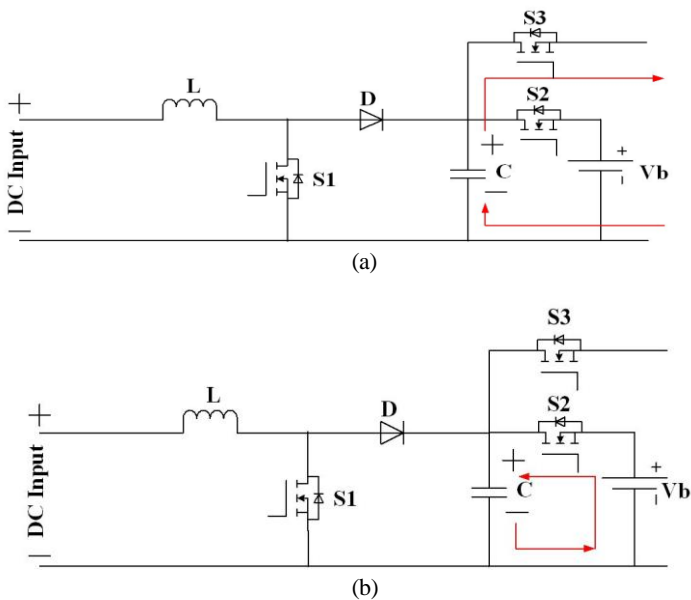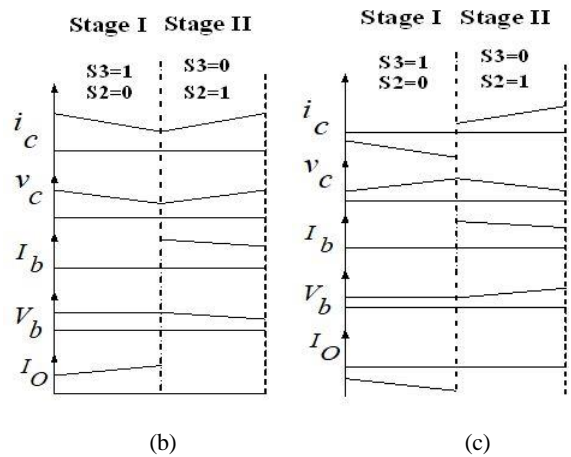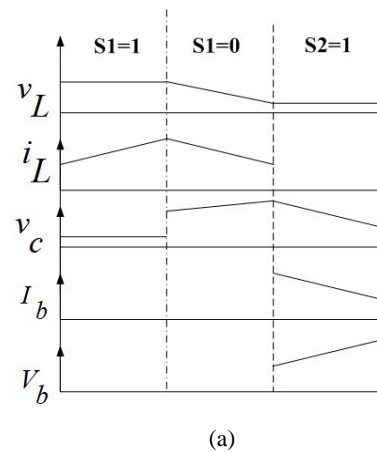Fig. 3. Regenerative operation during (a) Stage I (b) Stage II

(a)

(b)

(c)

Fig. 4. Relevant voltage and current waveform in different operation (a) Plug-in (b) Propulsion (c) Regenerative operation

(a)

(b)

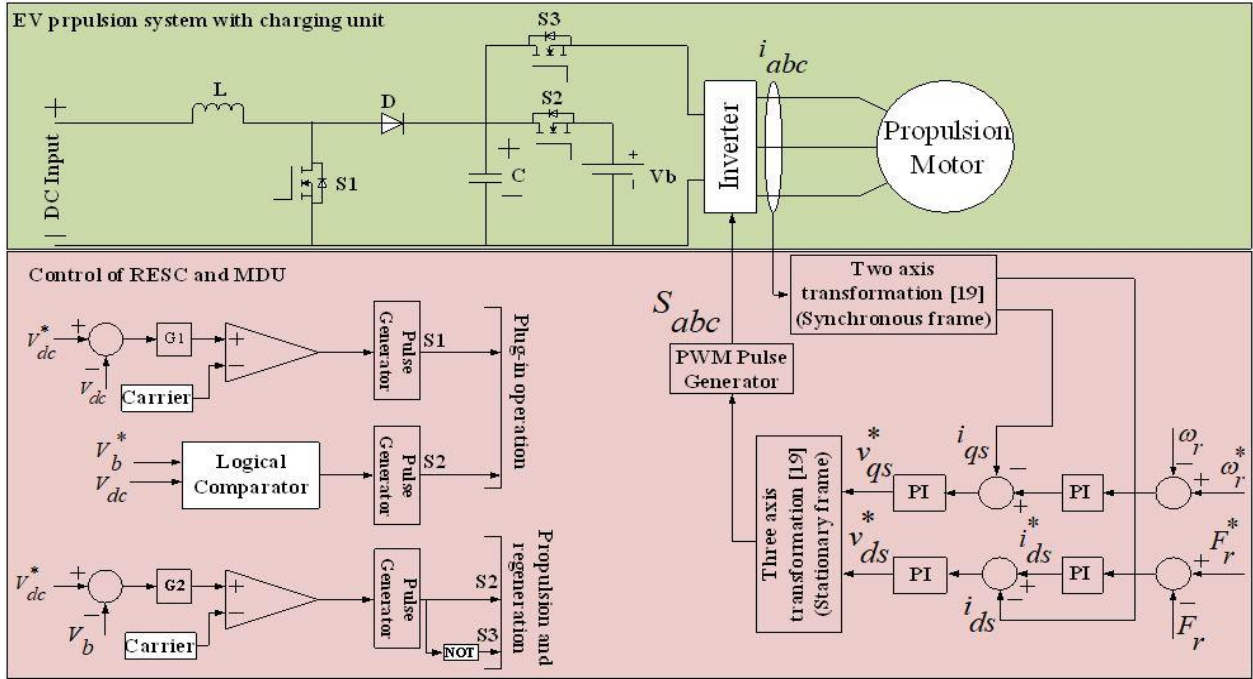Fig. 2. Propulsion operation during (a) Stage I (b) Stage II

Fig. 5. Complete system with control units for RESC and MDU

During stage II, this energy is then transferred to the connected battery and hence, the charging through the flow of current in path: $C^+ - S_2 - V_b^+ - V_b^- - C^-$. Flow of current path in stage I and II is shown in Fig. 3 (a) and Fig. 3 (b) respectively. Voltage-current waveforms during propulsion operation are shown in Fig. 4 (c).

4. Control strategies of system

Complete investigated system set-up together with their simplified control strategies is shown in Fig. 5. Control of the system set-up is constituted by the switching signal generation as discussed below:

4.1 RESC Control

For the operation of modified boost converter, DC-link voltage V_{dc} is compared with its reference value V_{dc}^* and error signal is fed to a proportional-integration (PI) controlled regulator G_1 to obtain the duty cycle. It is then fed to a comparator circuit wherein, a comparison with carrier signal is used to obtain the switching signal S_1 through a pulse generator. In RESC, the obtained DC link voltage V_{dc} is logically compared to the reference value of battery V_b^* as given below:

$if \ (V_{dc}^* > V_b)$

$S_2 = 1$

$else$

$S_2 = 0$

$end;$

Hence, switching signal S_2 is obtained through pulse generator. Further during propulsion and regeneration, battery voltage V_b is compared to the reference DC link V_{dc}^*. The generated voltage error is fed to a PI controlled regulator G_2 which is compared with the carrier signal and used to drive a pulse generator circuit to obtain the switching signal S_2. Switching signal S_3 is complimentary to S_2 and hence a NOT gate circuit is employed.

4.2 MDU Control

The concept of indirect field oriented control (FOC) has been utilized to achieve high performance of propulsion motor (three-phase induction motor). Indirect FOC is based on a decoupled control of flux and machine torque along two perpendicular axes (d-q axis). In this control, rotor field flux is assumed to align along d-axis whereas, current to control torque is along q-axis. Indirect FOC of induction motor is achieved in d-q axis frame of reference which is rotating at synchronous speed i.e. $\omega_k = \omega_e$. In order to achieve indirect FOC, motor equations are further simplified as given below:

Rewriting the rotor voltage-current relations along d-q axis yield,

$$0 = R_r i_{qdr} + (\omega_k - \omega_r)F_{dqr} + pF_{qdr} \tag{7}$$

where, rotor voltage is zero under steady-state i.e. $v_{qdr} = 0$. Slip speed ω_{sl} is defined as

$$\omega_{sl} = \omega_e - \omega_r \tag{8}$$

With the consideration of rotor field flux only along *d*-axis, we have

$$F_r = F_{dr} \tag{9}$$

$$F_{qr} = 0 \tag{10}$$

$$p\omega_r = 0 \tag{11}$$

After substitution of equations (9)-(11) in (7) and writing equation in *d-q* axis yields

$$R_{qr}i_{qr} + \omega_{sl}F_r = 0 \tag{12}$$

$$R_{dr}i_{dr} + pF_{dr} = 0 \tag{13}$$

Substitution of rotor current (i_{qr} and i_{dr}) from equation (4) in (12)-(13) results

$$\omega_{sl} = K_1 i_T \tag{14}$$

$$i_f = (1 + \tau_r p)F_r \tag{15}$$

where

$$K_1 = \frac{L_m}{\tau_r F_r} \tag{16}$$

$$i_T = i_{qs} \tag{17}$$

$$i_f = i_{ds} \tag{18}$$

$$\tau_r = \frac{L_r}{R_r} \quad \text{is rotor time constant} \tag{19}$$

Simplified torque after the substitution of rotor current yields

$$T_e = K_1 F_r i_T = K_2 i_T \tag{20}$$

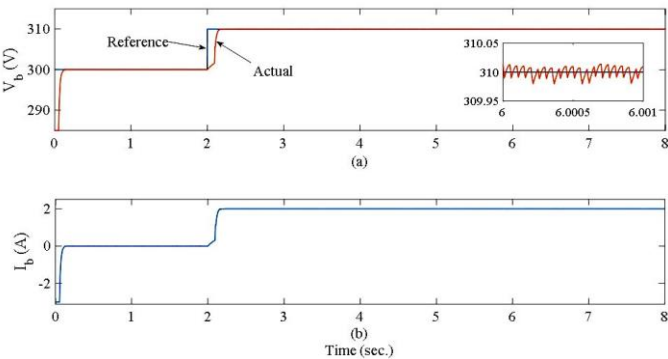$$K_1 = c\frac{L_m}{L_r} \tag{21}$$

$$K_2 = K_1 F_r \tag{22}$$

Fig. 6. Plug-in operation showing terminal condition of battery (a) voltage V_b (b) current I_b
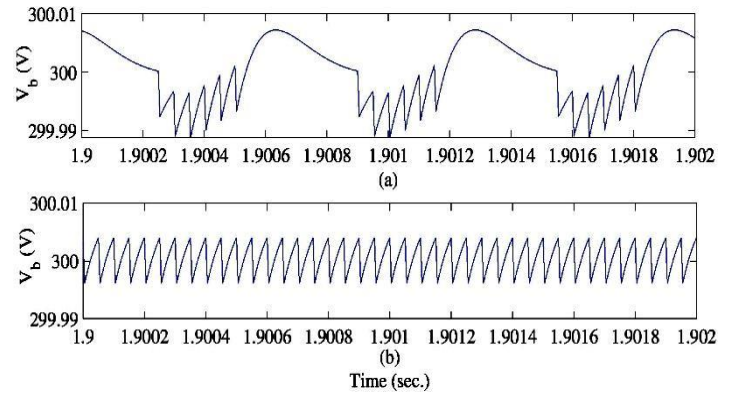

Fig. 7. Battery terminal voltage by using boost converter (a) with conventional topology (b) with proposed topology

Table 1. Parameters of induction machine

$r_s = 10\ \Omega$	$r_r = 6.3\ \Omega$
$L_{ls} = 0.04\ H$	$L_{lr} = 0.04\ H$
$L_m = 0.42\ H$	$J = 0.03\ Kgm^2$

5. Simulation results

The proposed boost converter topology is investigated under various operating modes applicable to EVs. Initially during plug-in operation, converter circuit is connected to a DC input at 240 V to regulate the DC link voltage to which a battery is connected. Battery is assumed to have the state of charge (SoC) at 95 % and 300 V as the nominal value. For charging purpose, DC link voltage should be higher than the terminal voltage of battery. Therefore, proposed boost converter is controlled initially at reference voltage i.e. 300 V. During the simulation process, this voltage was maintained for 2 sec. Further, after time $t = 2$ sec., reference voltage is boosted to 310 V. Change in the value of reference voltage is closely tracked by DC link voltage (which is connected to battery), as shown in Fig. 6 (a). A closed agreement of terminal voltage to the reference value is also shown in the same figure. Flow of the terminal current due to the difference in DC link voltage and battery is shown in Fig. 6 (b). In the converter circuit, value of inductor and capacitor are 31.5 *m*H, 62.5 μF respectively, which has been calculated as explained in [21]. Switching frequency of 150 kHz was used in converter operation. It is to be noted that the magnitude to harmonics are greatly reduced in comparison with their conventional counterpart as shown in Fig. 7 (a) and Fig. (b) respectively. However, a relatively higher frequency ripple was noted in voltage waveform of battery. Reduction in the magnitude in voltage harmonics will result in a higher lifetime of connected battery with reduced switching losses and, further signifies that proposed converter also mitigates the effect of secondary ripple/harmonics to much greater extent. Hence, the reduced effect of harmonics results in a higher efficiency with proposed converter topology.

In the propulsion system, a 2 HP, three-phase induction motor has been used whose parameters are given in Table 1. During the propul-

sion operation, load torque of 5 Nm. is given to a three-phase propulsion motor (i.e. induction motor) resulting in a small dip in rotor speed by 2 rad/sec. approximately. Initialization of propulsion is also
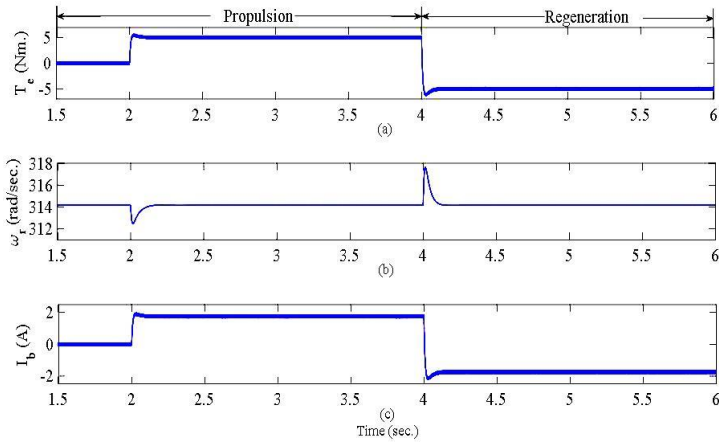

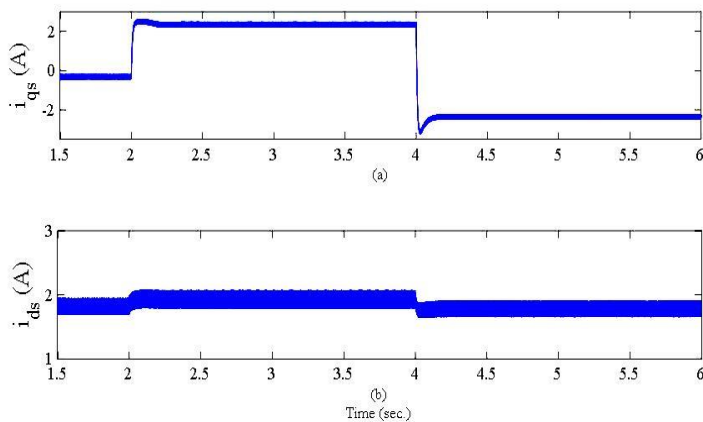Fig. 8. Propulsion and regeneration operation (a) developed torque (b) speed (c) input battery current

Fig. 9. Propulsion motor current in d-q axis (a) q-axis current i_{qs} (b) d-axis current i_{ds}
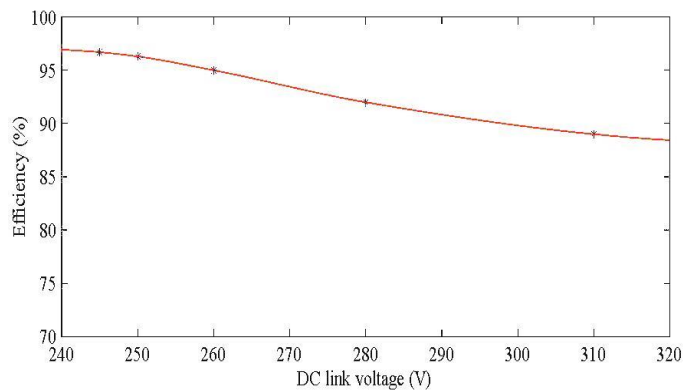

Fig. 10. Efficiency curve of proposed converter

accompanied by the increase in battery current I_b. During the propulsion operation, battery is assumed to operate at their nominal value. At

time $t = 4$ sec., direction of load torque is reversed with same magnitude (5 Nm.) to transit the operation to regeneration. This resulted in an eventual speed increase to 317.80 rad/sec. approximately, accompanied by the reversal of battery current. Speed response shows that the rotor regains the commanded reference value within a short time under the change in load torque both in propulsion and regeneration, signifying the disturbance rejection feature of motor drive. Machine developed torque, rotor speed and battery current in both propulsion and regeneration are shown in Fig. 8. (a), Fig. 8 (b) and Fig. 8 (c) respectively.

Connected propulsion motor current characteristic along d-q axes in both operation (propulsion and regeneration) is shown in Fig. 8. It may be noted that q-axis component, i.e. active component of stator current is changed from 2.33 A to -2.32 A (steady-state value) during propulsion and regeneration, respectively as shown in Fig 9 (a).

It may be noted that the PI type controllers G_1 and G_2 are regulated by tuning the value of K_{P1} and K_{I1} and, K_{P2} and K_{I2} respectively. Controllers G_1 and G_2 were operated during plug-in and regenerative operation, respectively. Tuning parameters of controller, proportional and integral constants K_P and K_I respectively, depend on the minimization of voltage error (i.e. $e_1 = V_{dc}^* - V_{dc}$; $e_2 = V_{dc}^* - V_b$). Tuned value of parameters used in simulation are $K_{P1} = K_{P2} = 0.0015$ and $K_{I1} = K_{I2} = 0.1$. Similarly, during propulsion operation, speed controller (K_{PS} and K_{IS}) and d-q voltage regulator (K_{PV} and K_{IV}) operate on the minimization of speed and current error (i.e. $e_3 = \omega_r^* - \omega_r$ and, $e_4 = i_{qs}^* - i_{qs}$ and $e_5 = i_{ds}^* - i_{ds}$). Value of the tuning parameter used in both speed and voltage regulator are: $K_{PS} = 2.5$, $K_{IS} = 65$ and, $K_{PV} = 580$, $K_{IV} = 50$ respectively.

In the analysis, motor is assumed to operate in constant torque region, i.e. speed not more than base value hence, flux level of machine is remain constant. Therefore, the value of d-axis component, i.e. reactive component of current was noted to be almost constant, as shown in Fig. 9 (b). Furthermore, the efficiency evaluation of proposed DC-DC boost converter is shown in Fig. 10. It may be noted that with increase in voltage level i.e. increase in duty cycle, a decreasing trend was found in converter efficiency. Decrease in efficiency is accounted by the increase in output voltage and hence the load current, resulting in higher conduction loss.

6. Conclusions

The paper presents a modified DC-DC boost converter topology which has been used to develop an integrated battery charging unit suitable for many applications. Developed charging unit has been in an EV to charge the connected battery during plug-in operation. The use of a nominal number for components signifies a simple and easy design of proposed converter circuit. Owing to the boost capability of converter, it may be used to charge the battery in wide voltage range. For this purpose, a simplified control scheme to regulate the voltage of DC link has been also developed. In the propulsion system, a three-phase induction motor has been used to operate the propulsion system during both propulsion and regeneration. In this system, indirect field oriented control scheme is used to ensure the high performance of propulsion system.

Present work may be extended to achieve an optimized operation by using an advanced sophisticated control mechanisms particularly, fuzzy logic, sliding mode, artificial neural network (ANN), model predictive control etc. [22-24].

Conflict of Interest Statement

The authors declare there is no conflict of interest in this study.

CRediT Author Statement

Amrita Kushwaha: Conceptualization, Writing-original draft,

Arif Iqbal: Conceptualization, Writing-original draft, writing-review & editing, validation, supervision,

M. Arifuddin Mallick: Writing-review & editing, supervision

References

[1] Chau KT. Electric vehicle machines and drives-design, analysis and application. Wiley; 2015.

[2] Zhang Y, Chen Z, Li G, Liu Y, Chen H, Cunn G, Early J. Machine learning-based vehicle model construction and validation—toward optimal control strategy development for plug-in hybrid electric vehicles. IEEE T Transp Electrif. 2022; 8(2):1590–1603. https://doi.org/10.1109/TTE.2021.3111966

[3] Yilmaz M, Krein PT. Review of battery charger topologies, charging power levels, and infrastructure for plug‐in electric and hybrid vehicles. IEEE T Power Electron. 2013; 28(5), 2151–2169. https://doi.org/10.1109/TPEL.2012.2212917

[4] Al‐Alawi BM, Bradley TH. Review of hybrid, plug‐in hybrid, and electric vehicle market modeling studies. Renew Sustain Energy Rev. 2013; 21, 190–203. https://doi.org/10.1016/j.rser.2012.12.048

[5] Mirza MS, Mohammad T, Alam Q, Mallick MA. Simulation and Analysis of a Grid Connected Multi-level Converter Topologies and their Comparison. J Electr Syst Inf Tech. 2014; 1 (2), 166-174. https://doi.org/10.1016/j.jesit.2014.07.007

[6] Shi C, Khaligh A. A two‐stage three‐phase integrated charger for electric vehicles with dual cascaded control strategy. IEEE J. Emerg. Sel. Topics Power Electron. 2018; 6(2), 898–909. https://doi.org/10.1109/JESTPE.2018.2797913

[7] Kuperman A, Levy U, Goren J, Zafransky A, Savernin A. Battery charger for electric vehicle traction battery switch station. IEEE T Ind Electron. 2013; 60(12), 5391–5399. https://doi.org/10.1109/TIE.2012.2233695

[8] Singh AK, Pathak MK. Single-phase bidirectional ac/dc converter for plug-in electric vehicles with reduced conduction losses. IET Power Electron. 2018; 11 (1), 140–148. https://doi.org/10.1049/iet-pel.2016.0899

[9] Singh AK, Pathak MK. Single-stage zeta-sepic-based multifunctional integrated converter for plug-in electric vehicles. IET Electr Syst Trans. 2018; 8 (2), 101–111. https://doi.org/10.1049/iet-est.2017.0063

[10] Singh AK, Pathak MK. A multi-functional single-stage power electronic interface for plug-in electric vehicles application. Electr Pow Compon Syst. 2018; 46 (2), 135–148. https://doi.org/10.1080/15325008.2018.1436619

[11] Chinmaya KA, Singh GK. Integrated onboard single-stage battery charger for PEVs incorporating asymmetrical six-phase induction machine. IET Electr Syst Trans. 2019; 9 (1), 8–15. https://doi.org/10.1049/iet-est.2018.5015

[12] Prasanna UR, Singh AK. Novel bidirectional single-phase single-stage isolated AC–DC converter with PFC for charging of electric vehicles. IEEE T Transp Electrific. 2017; 3 (3), 536–544. https://doi.org/10.1109/TTE.2017.2691327

[13] Saxena N, Hussain I, Singh B, Vyas AL. Implementation of a grid-integrated PV‐battery system for residential and electrical vehicle applications. IEEE T Ind Electron. 2018; 65(8), 6592–6601. https://doi.org/10.1109/TIE.2017.2739712

[14] Wang Z, Ching TW, Huang S, Wang H. Challenges faced by electric vehicle motors and their solutions. IEEE Access 2021; 9, 5228–5249. https://doi.org/10.1109/ACCESS.2020.3045716

[15] Muduli UR, Beig AR, Jaafari KA, Alsawalhi JY, Behera RK. Interrupt‐free operation of dual‐motor four‐wheel drive electric vehicle under inverter failure. IEEE T Transp Electrif. 2021; 7(1), 329–338. https://doi.org/10.1109/TTE.2020.2997354

[16] Cai W, Wu X, Zhou M, Liang Y, Wang Y. Review and development of electric motor systems and electric powertrains for new energy vehicles. Automot Innov. 2021; 4(1), 3–22. https://doi.org/10.1007/s42154-021-00139-z

[17] Mishra AK, Rajpurohit BS, Kumar R. Revampment of surface permanent magnet synchronous motor design for ameliorated torque profile in e‐mobility applications. IET Electr Syst Transp. 2021; 11 (2), 99–108. https://doi.org/10.1049/els2.12007

[18] Kumar S, Usman A, Rajpurohit BS. Battery charging topology, infrastructure, and standards for electric vehicle applications: A comprehensive review. IET Ener Syst Integ. 2021; 3 (4), 381-396. https://doi.org/10.1049/esi2.12038

[19] Iqbal A, Singh GK. Integrated battery charger of EVs using six-phase propulsion system. Electr Eng. 2023; 105, 2303–2317. https://doi.org/10.1007/s00202-023-01807-5

[20] Krause PC, Wasynczuk O, Sudhoff SD. Analysis of electrical machinery and drive systems. 2nd ed. Piscataway (NJ): IEEE Press; 2002/2004.

[21] Mohan N. Power electronics: a first course. Wiley, Hoboken; 2012.

[22] Balta G, Altin N, Nasiri A. Interval Type-2 Fuzzy-Logic-Based Constant Switching Frequency Control of a Sliding-Mode-Controlled DC–DC Boost Converter. Appl Sci. 2023; 13 (5), 3239. https://doi.org/10.3390/app13053239

[23] Boyacioglu NM, Kocakulak T, Batar M, Uyumaz A, Solmaz H. Modeling and Control of a PEM Fuel Cell Hybrid Energy System Used in a Vehicle with Fuzzy Logic Method. Int J Automot Sci Technol. 2023; 7 (4), 295-308. https://doi.org/10.30939/ijastech..1340339

[24] Yurdaer E, Kocakulak T. Comparison of Energy Consumption of Different Electric Vehicle Power Systems Using Fuzzy Logic-Based Regenerative Braking. Eng Perspect. 2021; 1 (1): 11-21. http://dx.doi.org/10.29228/sciperspective.47590